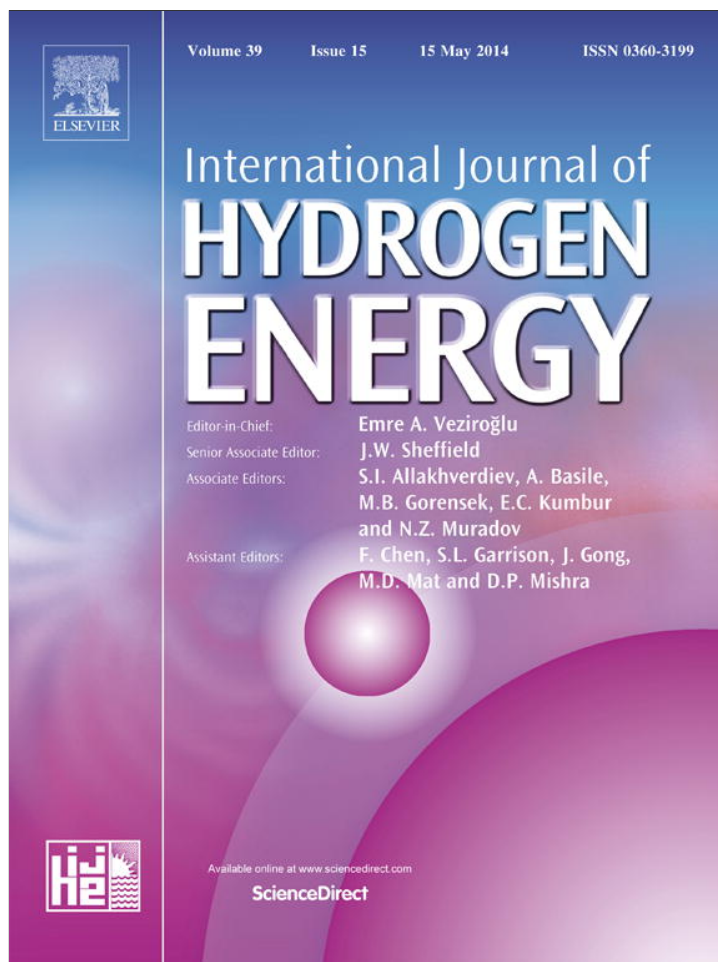


Provided for non-commercial research and education use.  
Not for reproduction, distribution or commercial use.



This article appeared in a journal published by Elsevier. The attached copy is furnished to the author for internal non-commercial research and education use, including for instruction at the authors institution and sharing with colleagues.

Other uses, including reproduction and distribution, or selling or licensing copies, or posting to personal, institutional or third party websites are prohibited.

In most cases authors are permitted to post their version of the article (e.g. in Word or Tex form) to their personal website or institutional repository. Authors requiring further information regarding Elsevier's archiving and manuscript policies are encouraged to visit:

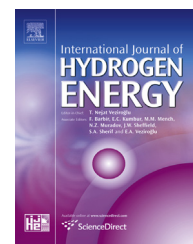
<http://www.elsevier.com/authorsrights>



ELSEVIER

Available online at [www.sciencedirect.com](http://www.sciencedirect.com)

ScienceDirect

journal homepage: [www.elsevier.com/locate/he](http://www.elsevier.com/locate/he)

# A well-dispersed catalyst on porous silicon micro-reformer for enhancing adhesion in the catalyst-coating process

Cheng-Chiang Huang<sup>a</sup>, Yuh-Jeen Huang<sup>a,\*</sup>, Hsueh-Sheng Wang<sup>b</sup>,  
Fan-Gang Tseng<sup>b</sup>, Yu-Chuan Su<sup>b</sup>

<sup>a</sup> Department of Biomedical Engineering & Environmental Sciences, National Tsing Hua University, Hsinchu 30013, Taiwan

<sup>b</sup> Department of Engineering and System Science, National Tsing Hua University, Hsinchu, Taiwan

## ARTICLE INFO

### Article history:

Received 31 December 2013

Received in revised form

28 February 2014

Accepted 9 March 2014

Available online 13 April 2014

### Keywords:

Coating

Microchannel

Partial oxidation of methanol

Hydrogen

## ABSTRACT

A Cu/Mn/ZnO catalyst slurry was modified with polyvinyl alcohol (PVA) as a dispersant and organic binder. The slurry, which forms a crack-free coating, was injected directly into an open microchannel before anodic bonding with Pyrex glass. To improve adherence, porous silicon (pore size  $<1 \mu\text{m}$ ) was fabricated in the microchannel. Ultrasonic vibration test (180 W, 20 min) showed good adhesion with only 6 wt.% loss. The thicker catalyst layer, with lower thermal diffusivity ( $0.98 \text{ mm}^2/\text{s}$ ), reduced heat loss during reaction on cratered design and performed better than two other geometric designs (blank, straight). The microchannel with cratered design can be deposited with a catalyst up to 24.4 mg, and has a hydrogen production rate of  $0.85 \text{ mmol h}^{-1}$  and 86% methanol conversion at  $200^\circ\text{C}$  under a feed rate of 2SCCM.

Copyright © 2014, Hydrogen Energy Publications, LLC. Published by Elsevier Ltd. All rights reserved.

## Introduction

Low-temperature, proton-exchange membrane fuel cells (PEMFCs) have been competitive candidates as power sources for portable devices, such as laptops and mobile phones. However, safely supplying and handling hydrogen are key issues for fuel cells. Among all the methods of hydrogen storage, hydrogen supplied from liquid fuels offers solutions to the problems of hydrogen storage and transportation.

Methanol's lower reforming temperature is suitable for portable devices [1]. Technology for converting methanol into

a hydrogen-rich supply for fuel cells is mainly based on steam reforming (SRM), partial oxidation (POM), or oxidative steam reforming (OSRM). While SRM is a familiar conversion pathway in most studies [2–4], it is limited by endothermic reaction. Heat needs to be supplied to sustain the reaction, but slow heat transfer in the catalytic bed results in slow response at start-up. Although OSRM reaction, the combination of POM and SRM, can be adjusted in a mild exothermic condition, it is more complicated to apply in a system. Among all the reactions, POM is one of the most promising for hydrogen production due to its low reforming temperature, energy savings, fast start-up and quick response of the whole system.

\* Corresponding author. Tel.: +88635715131x35496; fax: +88635718649.  
E-mail address: [yjhuang@mx.nthu.edu.tw](mailto:yjhuang@mx.nthu.edu.tw) (Y.-J. Huang).

Conventional packed-bed reactor has disadvantages, such as hot spots, delays in start-up, and mass and heat transfer limitations. For micro-scale reactor, the pressure drop is somewhat higher due to space constraints of channels being blocked with catalysts. A micro-pump used in portable applications may not be capable of overcoming a high pressure drop. On the other hand, microchannel reactor offers advantages, such as fast heating and cooling, large surface-area-to-volume ratios, and less energy input [5]. Some research has shown that wall-coated reactor performs better than packed-bed reactor for SRM reaction [6,7]. However, POM micro-reformer has never been reported in the literature.

The most common way to deposit catalysts within the microchannel is the wash-coating (slurry) technique. The advantage of wash-coating method is that it is a well-optimized catalyst that can be used directly. However, catalyst immobilization into microchannel has been a challenge, influenced by a low interaction between substrate surfaces and catalyst. Most research studies use inorganic binder to improve adherence. For commercial CuO/ZnO/Al<sub>2</sub>O<sub>3</sub> catalyst, alumina sol was often used as a binder [8,9]. Some researchers [10,11] also used ZrO<sub>2</sub> sol as binder to immobilize the catalyst onto a stainless steel microchannel. Nevertheless, using inorganic binder has some disadvantages. Chen et al. [12] reported that catalytic activity was significantly affected by the acidic sol because the catalysts were partially dissolved in the acidic slurry. Karim et al. [6] also mentioned that the low pH of the catalyst slurry caused catalyst dissolving. Lin et al. [13] also reported that catalyst activity decreases as the ratio of CeO<sub>2</sub> sol increases in the catalyst slurry. Thus, inorganic binder is not recommended because the catalyst's active regions may be covered by the inorganic sol [9,14,15].

In the present work, water was chosen as solvent because it is eco-friendly and cost less compared to organic-based slurry. However, the catalyst powder can easily agglomerate in water, which makes it impossible to form a crack-free catalyst coating. Some researchers [16–18] used hydroxyethyl cellulose to improve catalyst dispersion. Tadd et al. [19] used PVA and a ceria–zirconia binder to prepare the catalyst washcoat which then was ball-milled with zirconia grinding media for 48 h. Hwang et al. [9] used polyvinyl alcohol (PVA) as a drying, control chemical additive for pre-coated alumina adhesive layer. Peela et al. [20] used PVA and colloidal alumina for wash-coating  $\gamma$ -alumina on stainless steel microchannels. In this study, the catalyst surface was modified by adding PVA as dispersant to avoid the aggregation of particles and as binder for coating catalysts on the silicon microchannel.

Another strategy to enhance the adhesive strength is to use a pretreatment technique on substrate. Chemical treatment, such as sol–gel technique, is the most common method [21,22]. Kawamura et al. [18] deposited a thin Al<sub>2</sub>O<sub>3</sub> layer on the microchannel with a dip-coating method before catalyst loading. The other commonly used technique is surface modification on substrate. Anodic etching method is most often used in a substrate containing aluminum to obtain a porous alumina layer at the surface [23,24]. Compared to traditional catalyst support, such as porous ceramic material, coating a silicon substrate with a catalyst faces more challenges. Nevertheless, since silicon micro-reactors are light in weight and especially suitable for portable devices, an

effective method for surface modification of silicon is required. In this study, we used porous silicon to increase the adhesive strength between the catalyst layer and the microchannel. Pore size could be controlled by varying the parameters used for the formation of porous silicon, which is an efficient method to obtain spongy layers of silicon.

Additionally, different designs of microchannel reactor (straight, cratered, blank) have also been investigated to evaluate the effect of the geometries of microchannels on the catalytic performance. The possibility of using an open-channel coating method was demonstrated and compared to other coating methods, as well.

## Experimental

### Catalyst preparation

The Cu/Mn/ZnO catalysts were prepared by co-precipitation method. Copper, zinc, and manganese nitrates were added to deionized water, which was preheated to 70 °C, and then the nitrate precursors were stirred until they completely dissolved. The precipitating agent Na<sub>2</sub>CO<sub>3</sub> (2 M) was added while stirring the mixture until the solution reached a pH value of 8. The resulting precipitate was filtered by deionized water to remove the nitrate. The precipitate was dried at 105 °C overnight, and calcined at 400 °C for 4 h.

### Catalyst slurry preparation

PVA (87–90% hydrolyzed, average mol wt 30,000–70,000, SIGMA-ALDRICH) was added to deionized water first, and stirred at 70 °C until totally dissolved, then cooled at room temperature. As-synthesized, high-performance Cu/Mn/ZnO catalyst (10 wt.% catalyst) was added into the PVA solution (0.5 wt.%, 1 wt.%, 2 wt.% PVA) as-prepared. The catalyst slurry was kept in the ultrasonic bath for 1 h and then stirred at ambient temperature for 6 h.

### Porous silicon formation

The morphologies of porous silicon are modulated by several parameters including the doping and the resistivity of wafer, HF concentration, current density and etching time. In this research, the silicon wafers used for electrochemical etching were p-type with resistivity of 0.008–0.02  $\Omega$ -cm. The wafer was sliced into 2 cm  $\times$  2 cm pieces. Current densities varying from 1 mA/cm<sup>2</sup> to 40 mA/cm<sup>2</sup> (Electrochemical Analyzer, CH Instruments, model CHI730B) were applied on the wafers and microchannels. Etching solution was composed of HF (49%) and EtOH (99.7%) in different ratios and denoted by the concentration of HF. An etching time of between 10 min and 20 min was selected. Length of time determines the penetration depth of the pores in the substrate; i.e., deeper pores form with longer times. Since the pores obtained by electrochemical etching have an inverse cone shape, the pore diameter increases with the depth. Therefore, after the pore formation, the porous silicon was etched by NaOH solutions for 10–30 s in order to expose the rough and uneven pores.

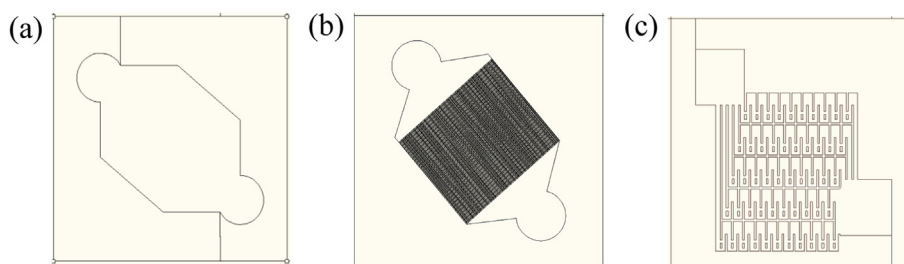


Fig. 1 – Various microchannel geometries; (a) blank design, (b) straight design, (c) cratered design.

### Characterization

The morphologies and thickness of catalyst and porous silicon were examined using both tungsten filament and field emission scanning electron microscope (FESEM). Rheology property was measured using a programmable rheometer (Brookfield MODEL DV-III). The pyrolysis temperature of PVA was measured by thermal analyzers (Setaram Labsys-TGDSC, DSC131). Thermal diffusivity of catalyst layer was measured by laser flash apparatus (LFA 447 NanoFlash<sup>®</sup>).

### Adhesion test

The silicon wafer was pre-treated before processing the adhesion test. First, the wafer was washed with 1:3 mixtures of the hydrogen peroxide and sulfuric acid for 10 min at 80 °C. The wafer surface was then washed with a 1:1:5 mixture of hydrogen peroxide, ammonia and deionized water for 10 min at 80 °C. Finally, the wafer was washed with 1:1:6 mixtures of the hydrogen peroxide, hydrochloric acid and deionized water for 10 min at 80 °C and then rinsed with the deionized water and dried at 80 °C. The wafer was treated by O<sub>2</sub> plasma for 60 s to increase the hydrophilicity before the catalyst slurry was deposited. After finishing the silicon wafer surface treatment, 20  $\mu$ l of catalyst slurry was dropped onto the wafer surface and dried at ambient temperature. Then the catalyst-coated wafer was calcined at 400 °C for 4 h. The adhesive strength of catalyst slurry on silicon wafer was estimated by ultrasonic vibration test. The wafer was kept in an ultrasonic bath (Rocker Ultrasonic cleaner Model: SONER 206H (180 W)) for 20 min. Weight loss was measured by balance (METTLER TOLEDO, XP105).

### Design of microchannel reactor

Various designs of the microchannel (straight, cratered, blank) were used to investigate the effect of the geometries in microchannel on catalytic performance. The schematic images of microchannels are shown in Fig. 1. The straight design with 144 channels offers the largest inner surface area for catalyst deposition. The cratered microchannel with longer channel length was designed to increase residence time for reactant gas and induce chaotic flow. Lastly, a blank design without any structure was used as reference. It has the smallest inner surface area. All of the microchannels were 350  $\mu$ m in depth. Their dimensions are summarized in Table 1.

### Microchannel reactor fabrication

A microchannel reactor was fabricated by deep reactive ion etching (DRIE) process. A thick photoresist (AZ 9260) was first spin-coated onto a silicon wafer (Fig. 2(a)). Next, by using a photolithography process and deep reactive ion etching (DRIE), desired shapes and depths on the silicon wafer were obtained (b). Then the thick photoresist was used as mask for porous silicon formation (c). The remaining photoresist was removed with piranha solution and O<sub>2</sub> plasma treatment was used to increase hydrophilicity, as well (d). Catalyst slurry was injected into the microchannel and dried as described later (e). Finally, anodic bonding technique was performed to bind the Pyrex glass and silicon together (f).

### Coating methods

In this study, flow-coating and open-channel injection methods were used for catalyst coating in microchannel. In the case of the flow-coating, or gas-displacement method [7,9], the microchannel was filled with the catalyst slurry, followed by the removal of excessive slurry by air and then dried at 120 °C for 10 min before the next loading. The coating process was repeated until reaching a desired amount of catalyst loading. In the open-channel injection technique, catalyst slurry was directly injected into open channel by a pipette. The catalyst-coated microchannels were dried at ambient temperature overnight, followed by drying at 120 °C for 1 h, then calcined at 400 °C for 4 h.

### Catalytic activity

#### Catalysis activity of packed-bed

Freshly calcined Cu/Mn/ZnO catalysts were grounded into fine powders, pressure-molded into granules, crushed and sieved from 60 to 80 mesh. The catalytic reactions were tested in a

Table 1 – Dimensions of microchannel reactor.

Geometry of microchannel	Blank	Straight	Cratered
Surface area	276.5 mm <sup>2</sup>	1048.8 mm <sup>2</sup>	457.8 mm <sup>2</sup>
Volume	47.1 mm <sup>3</sup>	32.3 mm <sup>3</sup>	48.4 mm <sup>3</sup>
Channel width	10 mm	30 $\mu$ m	400 $\mu$ m
Channel length	12 mm	8.5 mm	37 mm (average)
No. of channels	1	144	5

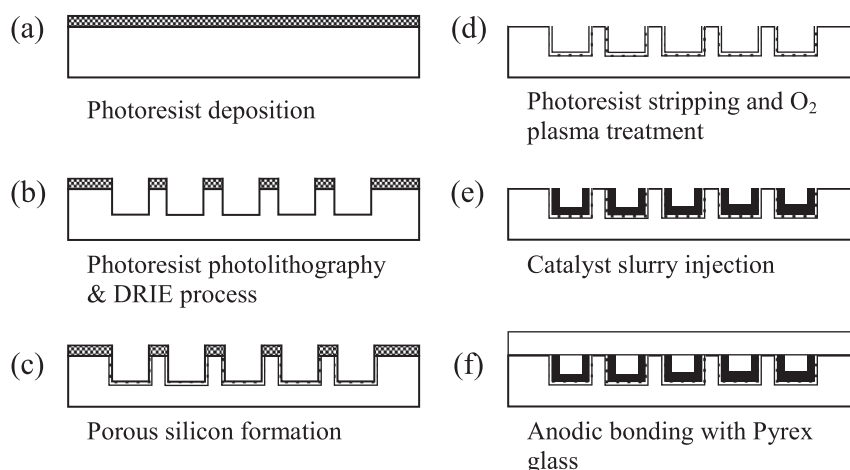


**Fig. 2 – Schematic of microreactor fabrication process.**

fixed-bed reactor (4 mm in id). Liquid methanol was fed into the pre-heater at a rate of 0.02 ml/min using liquid pump. The oxygen and argon flows were adjusted using mass flow controllers (Brooks). The reactant gases were methanol (12.2%) and oxygen (6.1%). Nitrogen (81.7%) was used as a carrier gas. Total flow was 100 ml/min. Under these conditions, the O<sub>2</sub>/CH<sub>3</sub>OH molar ratios in the feed were maintained at 0.5. The performance of the reactions over the catalysts was measured while raising the temperature from room temperature.

Reaction products were analyzed by a TCD-GC equipped with columns of Porapak Q (MeOH, CO<sub>2</sub> and H<sub>2</sub>O) and Molecular Sieve 5A (CO, O<sub>2</sub> and H<sub>2</sub>). Major products found in the performed reactions were H<sub>2</sub>, CO<sub>2</sub>, CO, and H<sub>2</sub>O. CH<sub>3</sub>OH conversion ( $C_{\text{MeOH}}$ ), H<sub>2</sub> selectivity ( $S_{\text{H}_2}$ ), and CO selectivity ( $S_{\text{CO}}$ ) are generally defined as:

$$C_{\text{MeOH}} = (n_{\text{MeOH, in}} - n_{\text{MeOH, out}}) / n_{\text{MeOH, in}} \times 100\%. \quad (1)$$

$$S_{\text{H}_2} = n_{\text{H}_2} / (n_{\text{H}_2\text{O}} + n_{\text{H}_2}) \times 100\% \quad (2)$$

$$S_{\text{CO}} = n_{\text{CO}} / (n_{\text{CO}_2} + n_{\text{CO}}) \times 100\% \quad (3)$$

#### Catalysis activity of microchannel reactor

The experimental set-up is the same as the one in fixed-bed except the tubular reactor was replaced by a microreactor and total flow rate of reactant gases was set at 2SCCM (SCCM denotes cubic centimeter per minute at STP) with a mass flow controllers (Brooks). The thermocouple reads the temperature at the center of the reactor's glass surface. Details of the microreactor housing assembly and the experimental set-up are shown in Fig. 3.

## Results and discussion

### Slurry characterization

Catalysts with various loading of Mn on CuZn-based catalysts were tested in a packed-bed reactor. As shown in Fig. 4(I), Cu<sub>30</sub>Mn<sub>20</sub>Zn catalyst shows optimum catalytic activity. Some

researchers [25,26] ascribe to the view that the electronic charge transfer between copper and manganese cations within the copper-manganese spinel lattice could enhance catalytic activity. The TPR profiles of Cu<sub>30</sub>Mn<sub>x</sub>ZnO catalysts (Fig. 4(II) (b) and (c)) also exhibit shoulders at a lower temperature range between 150 and 200 °C, which indicates that reducibility of catalysts could be improved by adding manganese promoter. Thus, Cu<sub>30</sub>Mn<sub>20</sub>ZnO catalysts were chosen in the following experiments.

PVA, as dispersant and binder, was used in this study for catalyst coating. The catalyst slurry was prepared simply from a mixture of catalyst powder and PVA in deionized water. Since the composition of catalyst slurry has a significant influence on coating properties, some fundamental characterizations of the catalyst slurry are presented. The stability of catalyst particles suspended in slurry was evaluated using optical images (Fig. 5(a) and (b)). Catalyst slurry (10 wt.%) without any additives was prepared for comparison. It was first put into ultrasonic bath for 1 h and then stirred for 48 h. In Fig. 5(a), agglomeration and sedimentation of catalyst particles in the slurry without PVA could be observed after standing for 4 h. Moreover, after being coated on silicon wafer, the catalyst layer cracked and could be peeled off easily, and parts of the silicon substrate were exposed (shown in Fig. 5(c)). On the contrary, as Fig. 5(b) shows, a well-dispersed suspension was obtained in a short time (1 h ultrasonic bath and 6 h magnetic stirring) in catalyst slurry with PVA. Moreover, a crack-free catalyst layer could be obtained when catalysts were coated on the silicon wafer, as shown in Fig. 5(d). The rheological properties of catalyst slurry are shown in Fig. 5(e). Catalyst slurry without PVA shows shear thinning behavior, whereas the rheological behavior of catalyst slurry with PVA is more like Newtonian fluid. The viscosity of catalyst slurry dispersed by PVA decreased two times compared to slurry without PVA. Since PVA could absorb onto catalyst particle surfaces, the long polymeric chains provided a steric stabilization to disperse particles and prevented agglomeration of catalyst particles. Thus, more stable suspension and smaller particles could be obtained, which also gave feedback to a lower viscosity behavior of catalyst slurry with PVA. The



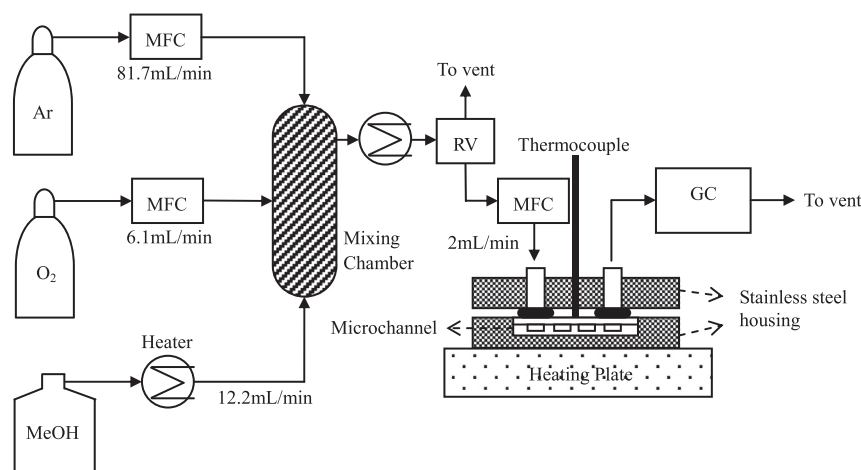


Fig. 3 – Experimental set-up for microchannel catalytic activity test.

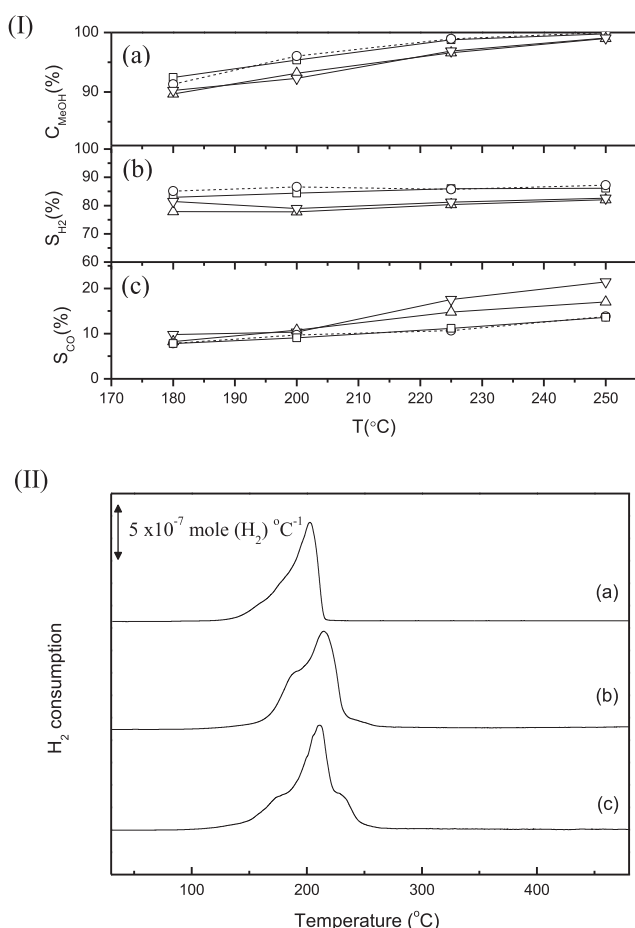


Fig. 4 – (I) (a) Methanol conversion, (b) hydrogen selectivity, and (c) carbon monoxide selectivity plotted vs. reaction temperature during POM reaction in packed-bed reactor for ( $\Delta$ )  $\text{Cu}_{30}\text{Zn}$ , ( $\nabla$ )  $\text{Cu}_{30}\text{Mn}_{10}\text{Zn}$ , ( $\square$ )  $\text{Cu}_{30}\text{Mn}_{20}\text{Zn}$ , ( $\circ$ ) calcined  $\text{Cu}_{30}\text{Mn}_{20}\text{Zn}$  catalyst slurry (10 wt.% cat., 2 wt.% PVA). (II) The  $\text{H}_2$ -TPR profiles of freshly  $\text{Cu}_{30}\text{Mn}_x\text{Zn}$  catalysts (a)  $\text{Cu}_{30}\text{Zn}$  (b)  $\text{Cu}_{30}\text{Mn}_{10}\text{Zn}$  (c)  $\text{Cu}_{30}\text{Mn}_{20}\text{Zn}$ .

relatively low viscosity of catalyst slurry also has the advantage of easily flowing through microchannel by capillary force, whereas non-dispersed slurry with high viscosity might block up the microchannel. Compared to using inorganic binder to prepare the catalyst slurry, this method is relatively simple and timesaving. The slurry with catalyst and PVA in the ratio of 5:1 shows good stability without flocculation for a few days and was used for the rest of the experiment.

According to the thermogravimetric analysis, PVA could be burned off completely below 400 °C. The performance of calcined  $\text{Cu}_{30}\text{Mn}_{20}\text{Zn}$  catalyst slurry (10 wt.% cat., 2 wt.% PVA) in Fig. 4(I) shows that the intrinsic activity of catalyst can be preserved after burning off PVA. The activity of catalyst slurry (10 wt.% cat., 2 wt.% PVA) was also tested in microchannel. Catalyst (3 mg) was loaded into the cratered design microchannel by flow-coating method and dried in an oven overnight. In Fig. 6, obviously, without removing PVA, the catalytic performance was dramatically low. This was because the active region was covered by PVA. Nevertheless, after loading catalyst slurry and the microchannel was calcined at 400 °C for 4 h to burn off PVA, the catalytic activity improved significantly. However, some catalyst layers easily peeled off under ultrasonic vibration test. To resolve this problem, surface modification on silicon wafer for increasing the adhesion of catalysts should be done.

#### Porous silicon formation

Porous silicon was used to increase the porosity and surface roughness in microchannel. For making porous silicon, the doping and the resistivity of the wafer significantly affects pore formation. It has been mentioned that p-type wafer with low resistivity often leads to micropores and n-type wafer will have macropores for the same resistivity ranges [27]. In addition, for n-type wafer, an illumination is necessary to promote the transfer of charge carriers between the solution and the substrate, which may cause the distribution of non-uniform pores. Therefore, p-type wafer with resistivity of 0.008–0.02  $\Omega\text{-cm}$  was selected for all the experiments in this study.

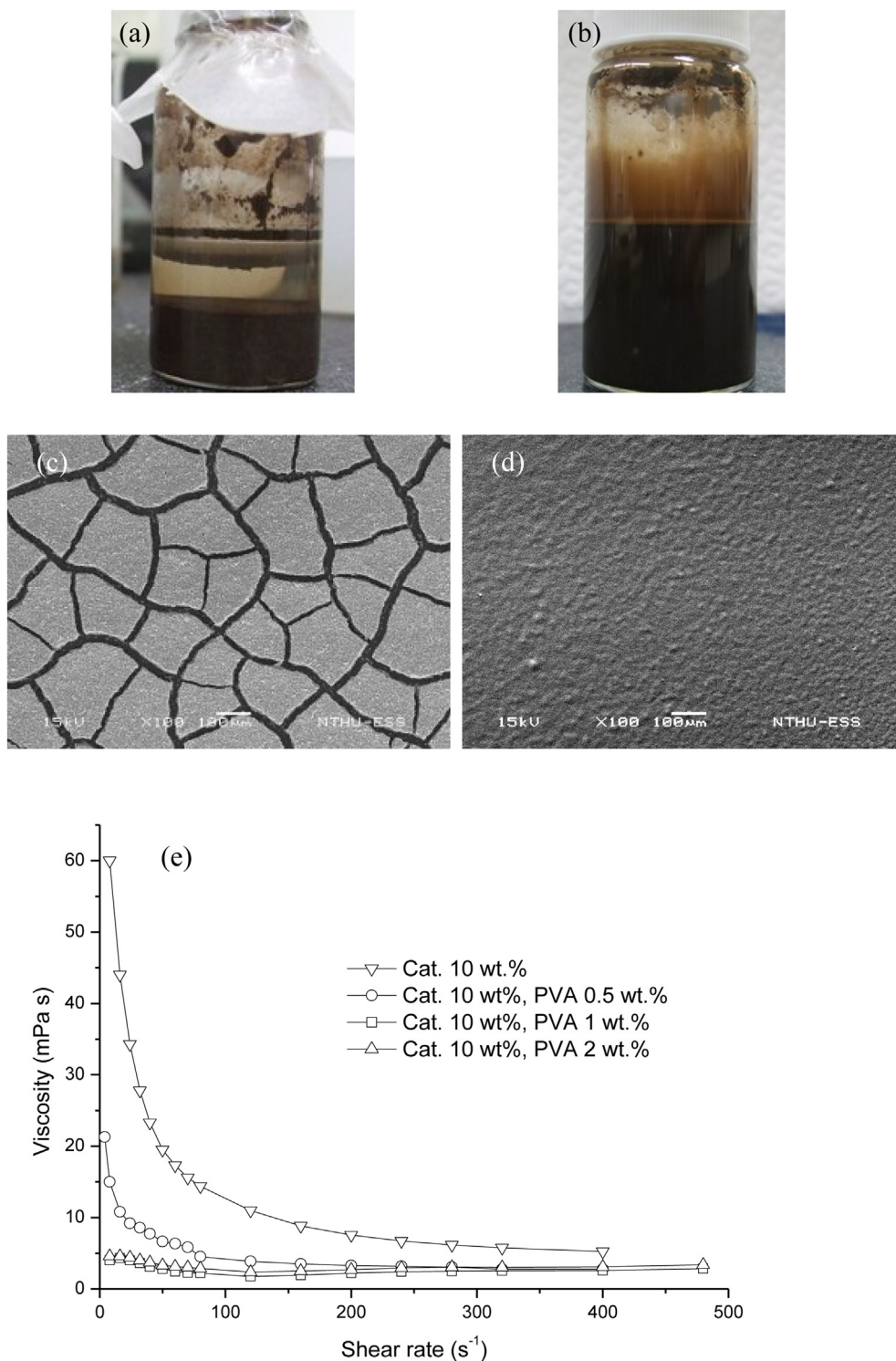


**Fig. 5 – Optical images of catalyst slurry; (a) 10 wt.% catalyst, (b) 10 wt.% catalyst, 2 wt.% PVA after standing for 4 h. SEM image of catalyst slurry coated on silicon substrate; (c) 10 wt.% catalyst, (d) 10 wt.% catalyst, 2 wt.% PVA. (e) Viscosity–shear rate curves of catalyst slurry with different concentration.**

First, bare silicon wafer was used for testing. Different HF concentration and current density were applied to modulate the pores and morphology in silicon and the results are shown in Fig. 7. Camara et al. [28] had used dry plasma etching to expose more pores and increase surface roughness in porous

silicon. In this study, NaOH solution was used for the same purpose, as shown in the upper right corner of Fig. 7(a). Fig. 7(b) shows the porous silicon with pore diameter between 100 and 400 nm, which was obtained under the condition of 20% HF, 10 mA/cm<sup>2</sup> current density for 600 s followed by 1 M

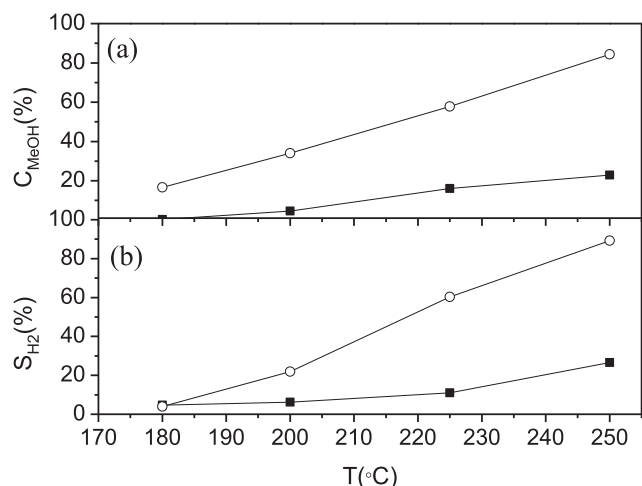


**Fig. 6 – (a) Methanol conversion, (b) hydrogen selectivity plotted vs. reaction temperature during POM reaction in microchannel reactor; (■) without calcination, (○) after calcination.**

NaOH etching for 20 s. After NaOH etching, the thickness of porous silicon was less than 1  $\mu\text{m}$ . The pore size increased with the current density as shown in Fig. 7(b) and (c). However, a high current density can cause an electropolishing of the substrate. Under 20% HF, as the current density increased to 40  $\text{mA}/\text{cm}^2$ , a non-uniform pore distribution resulted and some areas showed no pore formation. For fabricating porous silicon in microchannel, a longer time (900 s) is required to obtain uniform etching (shown in Fig. 7 (d) and (e)).

#### Adhesion test

Catalyst adherence is an important issue, especially in microchannel system. A detached catalyst may clog the microchannel, which can greatly increase the pressure drop and damage the whole power system. Ultrasonic vibration test is the most-used technique to evaluate the adhesion. The catalyst slurry (cat. 10 wt.%, PVA 2 wt.%) was first dropped onto the porous silicon wafer. After calcination, the wafer was kept in an ultrasonic bath (180 W) for 20 min to test catalyst adherence. Fig. 8(a) and (b) shows the SEM images of catalyst coat on porous silicon wafer after ultrasonic testing. A 9  $\mu\text{m}$ -thick catalyst layer remained on the porous structure wafer with average pore size around 100 nm, as shown in Fig. 8(b), and the weight loss was only 6 wt.%. For comparison, the same catalyst slurry was dropped on the bare wafer and about 78 wt.% calcined catalyst was lost during the ultrasonic test. This indicates that porous silicon can improve the adherence significantly. Fig. 8(c) shows the top surface of the catalyst layer. Average catalyst particle size is below 100 nm which is smaller than porous silicon pores. Thus, particles can fill the pores and an anchoring site is created by nano-sized pores that can interlock with the catalyst particles. Catalyst slurry without PVA was also dropped on the porous silicon. Without PVA, the catalyst might aggregate and form larger particle sizes which might influence the adhesion onto the substrate

[11,29,30]. As expected after ultrasonic testing, almost 85 wt.% catalyst was lost.

#### The catalytic performance in microchannel with different geometries

Three different microchannels (straight, cratered, blank) were fabricated, and the scales are shown in Table 1. The straight design provides the maximum number of channels (144) and surface area (1048.8  $\text{mm}^2$ ), and was expected to have the best catalytic performance originally. The cratered microchannel provides the longer channel length (37 mm), and the blank design with no structure (276.5  $\text{mm}^2$  and 12 mm) was used as reference. All three designs were loaded repeatedly until reaching the same expected amount ( $\sim 9$  mg) of catalyst by flow-coating method. The results of catalytic performance during POM reaction in these three different microchannels are shown in Fig. 9(I). All three designs can achieve over 95% methanol conversion at  $T > 225$   $^{\circ}\text{C}$ . It can be seen that the surface area of 276.5  $\text{mm}^2$  and 12 mm channel length in blank design is sufficient for full methanol conversion under the feed rate of 2SCCM. However, even though the straight design has the highest surface area (1048.8  $\text{mm}^2$ ), the  $C_{\text{MeOH}}$  dropped to 38% at 200  $^{\circ}\text{C}$  for both of straight and blank design, but it could be kept to 63% at 200  $^{\circ}\text{C}$  for the cratered design. As shown in Fig. 9(II), the catalyst layer in cratered design was concentrated on one side of the microchannel due to the force of air by flow-coating and had an average thickness of 19  $\mu\text{m}$  on the wall and over 70  $\mu\text{m}$  at the corner. The straight design was coated with 4–6  $\mu\text{m}$  thick catalyst on the wall and the blank design was coated with 16–30  $\mu\text{m}$  thick on the bottom. Tang et al. [31] mention that catalyst can act as a temporary thermal storage for autothermal reaction in packed-bed reactor. When it comes to microchannel reactor, a thicker catalyst layer can prevent heat loss, as well. In this study, the thermal diffusivity of catalyst layer and silicon wafer, as measured by flash method, were 0.98  $\text{mm}^2/\text{s}$  and 31.44  $\text{mm}^2/\text{s}$ , respectively. Since thermal diffusivity represents the rate of heat flow through matter, the low thermal diffusivity of the catalyst means it is a good material for preserving heat. For microchannel with a thin catalyst layer, heat generated from the POM reaction can be transferred easily to the surroundings, and results in a smaller temperature gradient in microchannel. Since catalytic performance is very sensitive to temperature, it could decrease significantly in straight design microchannel at lower temperature. Compared to the other two designs, the cratered microchannel design may have the highest temperature at the center of the reaction zone because it has the thickest catalyst layer at the corner of microchannel, which results in the highest catalytic performance at lower reaction temperature.

#### Comparison between different coating methods

At first, fill-and-dry method was used for catalyst coating, but longer times for evaporation of the water through the small inlet ports and the outlet were needed. Besides, a non-uniform distribution of catalyst layer formed because the slurry flowed towards the inlets and the outlet of the microchannel during the drying step. Thus, flow-coating method which uses



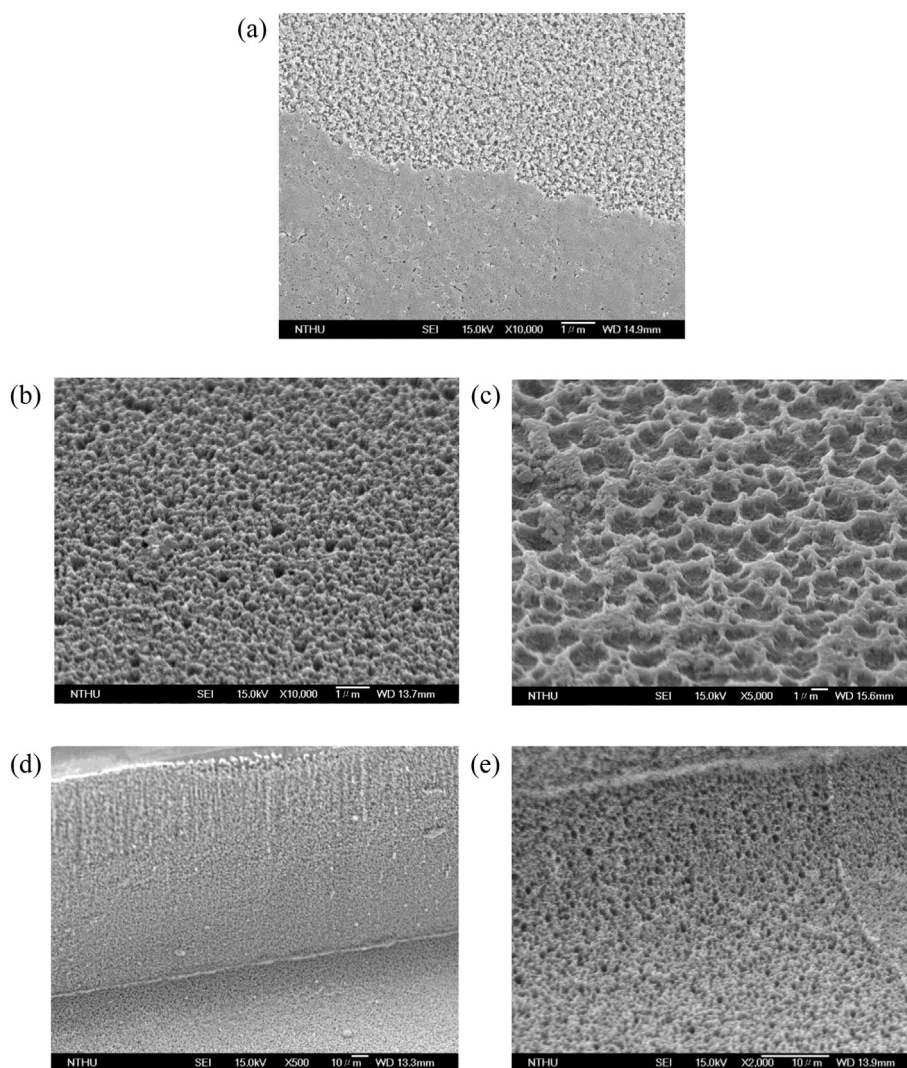


**Fig. 7 – SEM image of porous silicon under different conditions; (a) 15% HF, 1 mA/cm<sup>2</sup>, 600 s, followed by 0.1 M NaOH etched for 20 s, (b) 20% HF, 10 mA/cm<sup>2</sup>, 600 s, followed by 1 M NaOH etched for 20 s, (c) 20% HF, 40 mA/cm<sup>2</sup>, 600 s, followed by 1 M NaOH etched for 20 s, (d) 20% HF, 10 mA/cm<sup>2</sup>, 900 s, followed by 1 M NaOH etched for 20 s in microchannel, (e) magnification of the image shown in (d).**

compressed gas to remove the excess slurry was used in this study [7]. In addition, better adhesion of catalyst was obtained especially for the thicker catalyst layer due to the extra force exerted on the catalyst layer by the flow of compressed gas. By flow-coating method, the maximum amount of catalyst (21.0 mg) could be loaded in the microchannel with cratered design. However, some catalyst slurry was wasted and catalyst blocking at inlets may occur after several loadings.

Open-channel coating was also used in this research. It was more convenient because drying the catalyst slurry in the open-channel was faster, and a more-uniform catalyst layer could be obtained. However, if contamination formed on the top surface of open microchannel during the catalyst coating process, the anodic bonding process may fail and gas leakage may occur. Many researchers have reported using a mask or sacrificial layer for selective open-channel catalyst coating [18,32,33], and the mask could be removed during the calcination step. Kim et al. [34] mentioned that as the ratio of

thickness to width of the catalyst layer on the sacrificial layer is more than 0.03, the catalyst layer was not easily removed after decomposition of sacrificial layer. In this study, the well-dispersed catalyst slurry could be directly injected into microchannel without overflowing onto the top surface. This technique showed no problem in the anodic bonding process and can be used in microchannel with a depth deeper than 200 μm when using catalyst slurry with solid content up to 20 wt.%. Fig. 10(I) shows the EDX-mapping of catalyst loading in microchannel with a 200 μm depth. It is evidence that the catalyst was only coated in microchannel. For cratered microchannel, 24.4 mg can be loaded by open-channel coating, but cracking was hard to avoid at the region with a very thick catalyst layer [29].

Fig. 10(II) shows the catalyst activity in cratered microchannel of these two different coating methods. The result shows no specific difference in performance between the two coating methods. While, open-channel injection method is

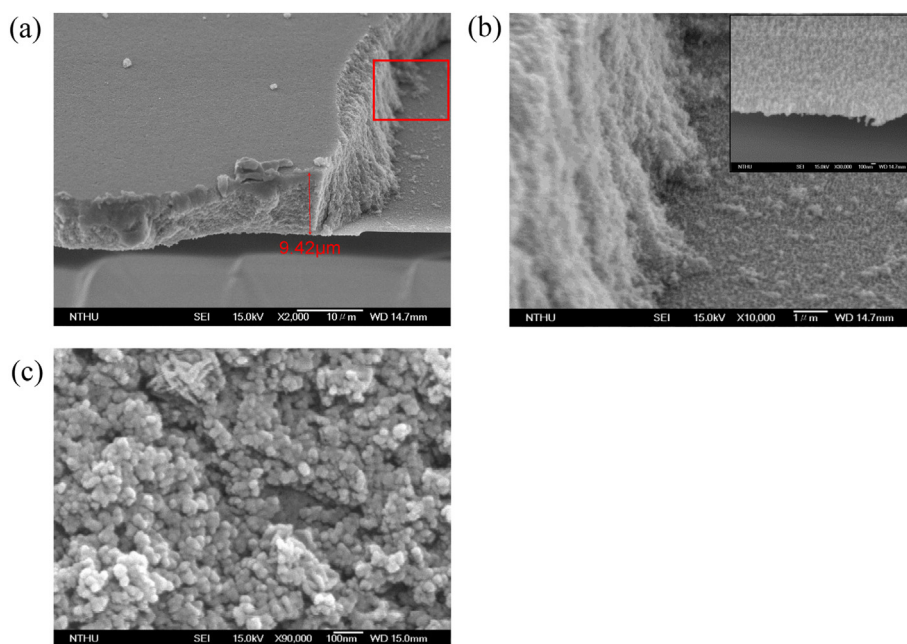


Fig. 8 – SEM image of (a) catalyst coated silicon substrate after ultrasonic test, (b) magnification of the image shown in (a), (c) top surface of catalyst layer.

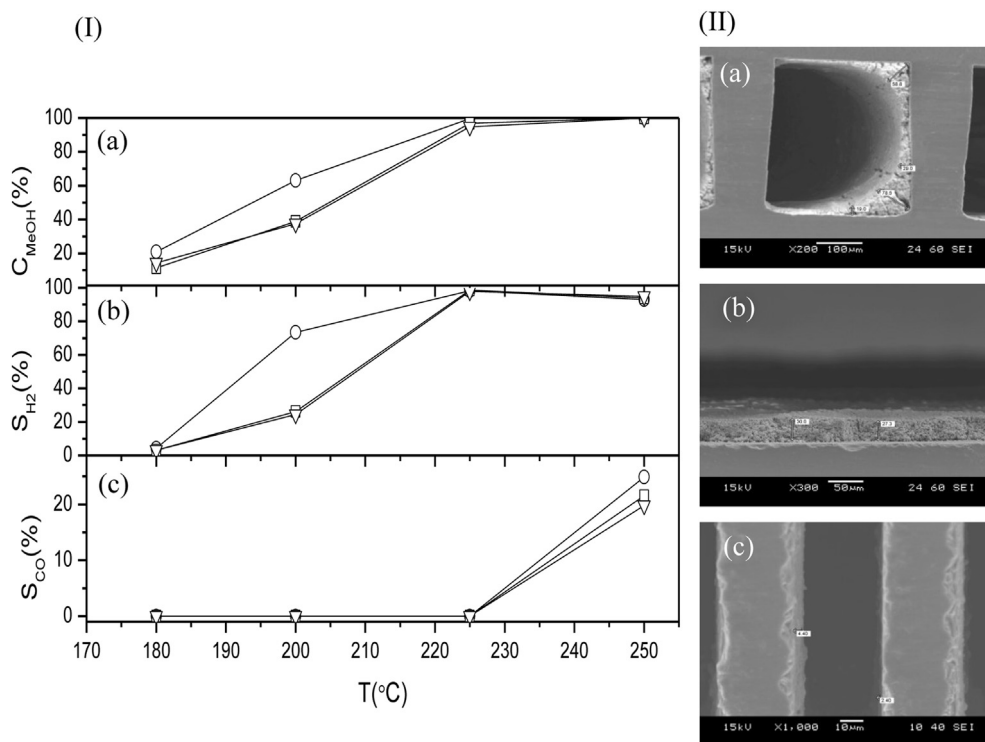
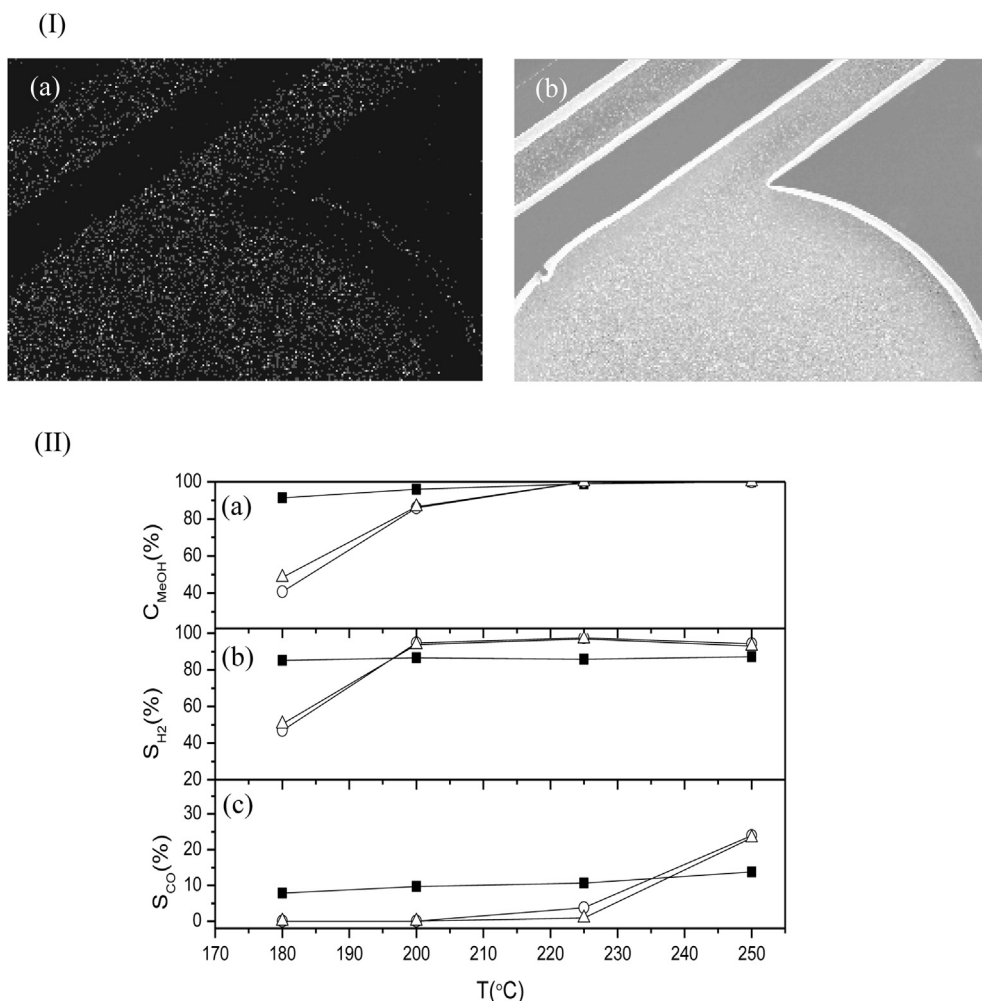


Fig. 9 – (I) (a) Methanol conversion, (b) hydrogen selectivity, and (c) carbon monoxide selectivity plotted vs. reaction temperature during POM reaction in microchannel reactor; (c) cratered design (9.3 mg), (□) blank design (9.3 mg), (▽) straight design (9.0 mg). (II) SEM image of catalyst layer coated in microchannel reactor; (a) cratered design, (b) blank design, (c) straight design.



**Fig. 10 – (I) EDX-analysis of microchannel with depth of 200  $\mu\text{m}$ . (a) Cu K $\alpha$ , (b) SEM image of microchannel. (II) (a) Methanol conversion, (b) hydrogen selectivity, and (c) carbon monoxide selectivity plotted vs. reaction temperature during POM reaction; ( $\Delta$ ) close-channel flow-coating method, ( $\circ$ ) open-channel injection method in cratered microchannel reactor, ( $\blacksquare$ ) dried catalyst slurry (10 wt.% cat., 2 wt.% PVA) followed by calcination at 400 °C for 4 h in packed-bed reactor.**

more efficient and facilitates mass production, flow-coating method provides better adhesion of catalyst layer in microchannel.

#### Comparison between the performance of packed-bed reactor and microchannel

It is worth mentioning that catalytic performance in microchannel is lower than that in packed-bed at lower temperature even though the catalyst loading is sufficient in microchannel as shown in Fig. 10(II). Since silicon has excellent thermal conductivity, the silicon microchannel and the surroundings can be thought of as a heat sink [35] and can smooth out the temperature gradient in an exothermic microchannel, thereby causing a decrease in catalytic performance. The microchannel with thicker catalyst coating may still suffer from heat loss to the environment. In our calculations, the heat generated from POM reaction per min under the feed rate of 2SCCM can increase the temperature of the silicon microchannel, which is only 0.35 g up to 4.9 °C under adiabatic conditions. Tadd et al. [19] have also shown that the thermal-insulated microchannel

has higher performance than a standard one for autothermal reforming of isooctane.

However, the excellent heat transfer ability of silicon could also be an advantage. Local hot spots can be avoided by removing heat through the silicon microchannel; and thus, forming less CO by the endothermic r-WGS reaction at lower temperatures [36]. It can be seen that no CO was detected for microchannel with 9 mg catalyst loading in the range of 180–225 °C in Fig. 9(I) and the CO selectivity was only 3.7% for microchannel with 24.4 mg catalyst loading at 225 °C in Fig. 10(II). On the contrary, the CO selectivity of packed-bed reactor was almost 10% or higher at all temperatures measured. Thus, thermal management would play a critical role in building a high-performance microchannel at low-temperature.

#### Conclusion

In this research, we demonstrate the possibility of using PVA to modify the surface of Cu/Mn/ZnO catalyst. The catalyst



slurry in a ratio of 5:1 (Catalyst:PVA) shows excellent dispersion and good adhesion to the silicon substrate. No mask or sacrificial layer on the top surface is required when catalyst slurry is directly loaded into open microchannel. This could simplify the fabrication procedure. In addition, the catalyst preserves its intrinsic activity after calcination. Furthermore, porous silicon was used to enhance the adherence between catalyst layer and microchannel. Pore size below 1  $\mu\text{m}$  can be obtained under the condition of 20% HF, 10 mA/cm<sup>2</sup> current density and etched for 600 s followed by 1 M NaOH etching for a P-type silicon wafer. The catalyst layer dropped by slurry with 10 wt.%, catalyst and 2 wt.% PVA shows good adhesion on porous silicon with only 6 wt.% loss in the ultrasonic vibration test (180 W, 20 min). This may be attributed to the micropores of porous silicon which can interlock with the catalyst particles.

In the activity test, partial oxidation of methanol (POM) reaction was used in the microchannel. Among three different microchannel geometries with the same catalyst loading, the cratered design shows better catalytic performance over the other two designs because of its thicker catalyst layer. The thicker catalyst layer with low thermal diffusivity (0.98 mm<sup>2</sup>/s) can reduce heat loss to the surroundings. For microchannel with cratered design, up to 21 mg and 24.4 mg catalyst loading can be obtained by flow-coating method and open-channel injection method, respectively. The microchannel has a hydrogen production rate of 0.85 mmol h<sup>-1</sup> and 86% methanol conversion at 200 °C under the flowing rate of 2SCCM.

Packed-bed reactor with its high thermal resistance property can preserve the heat generated from the exothermic POM reaction in the catalyst and has higher energy efficiency and performance. However, high CO content in the product gas and the pressure drop of packed-bed reactor may become a serious problem for portable fuel cells. Silicon microchannel with its high thermal conductivity can avoid the problem of hot spots and thus reduce CO formation at lower temperature ( $T < 230$  °C). With better heat management, we believe POM microchannel can be a competitive option as a hydrogen source for PEMFC. Several adjustments, such as thermal insulation and redesign of microchannel, should be done to optimize the performance and improve the energy efficiency of microchannel in the future.

## Acknowledgments

The authors are grateful for the financial support of this work from the Ministry of Science and Technology of Taiwan (101-2221-E-007-083-).

## REFERENCES

- [1] Brown LF. A comparative study of fuels for on-board hydrogen production for fuel-cell-powered automobiles. *Int J Hydrogen Energy* 2001;26(4):381–97.
- [2] Udani PPC, Gunawardana PVDS, Lee HC, Kim DH. Steam reforming and oxidative steam reforming of methanol over CuO-CeO<sub>2</sub> catalysts. *Int J Hydrogen Energy* 2009;34(18):7648–55.
- [3] Suh JS, Lee MT, Greif R, Grigoropoulos CP. Transport phenomena in a steam-methanol reforming microreactor with internal heating. *Int J Hydrogen Energy* 2009;34(1):314–22.
- [4] Lee MT, Greif R, Grigoropoulos CP, Park HG, Hsu FK. Transport in packed-bed and wall-coated steam-methanol reformers. *J Power Sources* 2007;166(1):194–201.
- [5] Ouyang X, Bednarova L, Besser RS, Ho P. Preferential oxidation (PrOx) in a thin-film catalytic microreactor: advantages and limitations. *Aiche J* 2005;51(6):1758–72.
- [6] Karim A, Bravo J, Gorm D, Conant T, Datye A. Comparison of wall-coated and packed-bed reactors for steam reforming of methanol. *Catal Today* 2005;110(1–2):86–91.
- [7] Bravo J, Karim A, Conant T, Lopez GP, Datye A. Wall coating of a CuO/ZnO/Al<sub>2</sub>O<sub>3</sub> methanol steam reforming catalyst for micro-channel reformers. *Chem Eng J* 2004;101(1–3):113–21.
- [8] Park GG, Seo DJ, Park SH, Yoon YG, Kim CS, Yoon WL. Development of microchannel methanol steam reformer. *Chem Eng J* 2004;101(1–3):87–92.
- [9] Hwang SM, Kwon OJ, Kim JJ. Method of catalyst coating in micro-reactors for methanol steam reforming. *Appl Catal A Gen* 2007;316(1):83–9.
- [10] Lim MS, Kim MR, Noh J, Woo SI. A plate-type reactor coated with zirconia-sol and catalyst mixture for methanol steam-reforming. *J Power Sources* 2005;140(1):66–71.
- [11] Kundu A, Park JM, Ahn JE, Park SS, Shul YG, Han HS. Micro-channel reactor for steam reforming of methanol. *Fuel* 2007;86(9):1331–6.
- [12] Chen KY, Shen CC, Lee CY, Lee SJ, Leu CH, Wang JH, et al. Coating powdered copper catalyst with yttria sol. *Mater Chem Phys* 2011;128(1–2):57–61.
- [13] Lin KS, Chowdhury S, Yeh HP, Hong WT, Yeh CT. Preparation and characterization of CuO/ZnO-Al<sub>2</sub>O<sub>3</sub> catalyst washcoats with CeO<sub>2</sub> sols for autothermal reforming of methanol in a microreactor. *Catal Today* 2011;164(1):251–6.
- [14] Nijhuis TA, Beers AEW, Vergunst T, Hoek I, Kapteijn F, Moulijn JA. Preparation of monolithic catalysts. *Catal Rev* 2001;43(4):345–80.
- [15] Patil MD, Lachman IM. Methanol conversion on ceramic honeycombs coated with silicalite. *ACS Symp Ser* 1988;368:492–9.
- [16] Pfeifer P, Schubert K, Liauw MA, Emig G. PdZn catalysts prepared by washcoating microstructured reactors. *Appl Catal a-Gen* 2004;270(1–2):165–75.
- [17] Pfeifer P, Schubert K, Emig G. Preparation of copper catalyst washcoats for methanol steam reforming in microchannels based on nanoparticles. *Appl Catal A Gen* 2005;286(2):175–85.
- [18] Kawamura Y, Ogura N, Yamamoto T, Igarashi A. A miniaturized methanol reformer with Si-based microreactor for a small PEMFC. *Chem Eng Sci* 2006;61(4):1092–101.
- [19] Tadd AR, Gould BD, Schwank JW. Packed bed versus microreactor performance in autothermal reforming of isooctane. *Catal Today* 2005;110(1–2):68–75.
- [20] Peela NR, Mubayi A, Kunzru D. Washcoating of gamma-alumina on stainless steel microchannels. *Catal Today* 2009;147:S17–23.
- [21] Stefanescu A, van Veen AC, Mirodatos C, Beziat JC, Duval-Brunel E. Wall coating optimization for microchannel reactors. *Catal Today* 2007;125(1–2):16–23.
- [22] Younes-Metzler O, Svagin J, Jensen S, Christensen CH, Hansen O, Quaade U. Microfabricated high-temperature reactor for catalytic partial oxidation of methane. *Appl Catal A Gen* 2005;284(1–2):5–10.
- [23] Koo KY, Joo H, Jung UH, Choi EJ, You SM, Yoon WL. Novel surface pretreatment for metal structured catalyst. *Catal Today* 2011;164(1):52–7.
- [24] Leon MA, Tschentscher R, Nijhuis TA, van der Schaaf J, Schouten JC. Rotating foam stirrer reactor: effect of catalyst



- coating characteristics on reactor performance. *Ind Eng Chem Res* 2011;50(6):3184–93.
- [25] Kanungo SB. Physicochemical properties of MnO<sub>2</sub> and MnO<sub>2</sub>–CuO and their relationship with the catalytic activity for H<sub>2</sub>O<sub>2</sub> decomposition and Co oxidation. *J Catal* 1979;58(3):419–35.
- [26] Figueroa SJA, Requejo FG, Lede EJ, Lamaita L, Peluso MA, Sambeth JE. XANES study of electronic and structural nature of Mn-sites in manganese oxides with catalytic properties. *Catal Today* 2005;107-08:849–55.
- [27] Camara EHM, Breuil P, Briand D, Guillot L, Pijolat C, de Rooij NF. Micro gas preconcentrator in porous silicon filled with a carbon absorbent. *Sens Actuators B Chem* 2010;148(2):610–9.
- [28] Pijolat C, Camara M, Courbat J, Viricelle JP, Briand D, de Rooij NF. Application of carbon nano-powders for a gas micro-preconcentrator. *Sens Actuators B Chem* 2007;127(1):179–85.
- [29] Agrafiotis C, Tsetsekou A, Ekonomakou A. The effect of particle size on the adhesion properties of oxide washcoats on cordierite honeycombs. *J Mater Sci Lett* 1999;18(17):1421–4.
- [30] Agrafiotis C, Tsetsekou A. The effect of powder characteristics on washcoat duality. Part I: alumina washcoats. *J Eur Ceram Soc* 2000;20(7):815–24.
- [31] Tang HY, Erickson P, Yoon HC, Liao CH. Comparison of steam and autothermal reforming of methanol using a packed-bed low-cost copper catalyst. *Int J Hydrogen Energy* 2009;34(18):7656–65.
- [32] Chen H, Bednarova L, Besser RS, Lee W. Surface-selective infiltration of thin-film catalyst into microchannel reactors. *Appl Catal A Gen* 2005;286(2):186–95.
- [33] Kim T, Lee DH, Park DE, Kwon S. Micromachined methanol reformer for portable PEM fuel cells. *J Fuel Cell Sci Tech* 2008;5(1).
- [34] Kim T, Kwon S. Catalyst preparation for fabrication of a MEMS fuel reformer. *Chem Eng J* 2006;123(3):93–102.
- [35] Srinivas S, Dhingra A, Im H, Gulari E. A scalable silicon microreactor for preferential CO oxidation: performance comparison with a tubular packed-bed microreactor. *Appl Catal A Gen* 2004;274(1–2):285–93.
- [36] Ouyang X, Besser RS. Effect of reactor heat transfer limitations on CO preferential oxidation. *J Power Sources* 2005;141(1):39–46.